# The electronic properties of intermetallic hydrides with the $K_2PtCl_6$ structure



1993 J. Phys.: Condens. Matter 5 6697

(http://iopscience.iop.org/0953-8984/5/36/025)

J. Phys.: Condens. Matter 5 (1993) 6697–6718. Printed in the UK

# The electronic properties of intermetallic hydrides with the $K_2PtCl_6$ structure

Emilio Orgaz and Michèle Gupta

Institut de Science des Matériaux, URA-446, Bâtiment 415, Université de Paris-Sud, 91405 Orsay Cédex, France

Received 15 April 1993, in final form 18 June 1993

**Abstract.** In this paper we present our results from electronic structure calculations of the intermetallic hydrides $M_2M'H_6$ (M=Mg, Ca, Sr, M'= Fe, Ru, Os). Most of these hydrides have been recently synthesized and characterized, all showing the $K_2PtCl_6$ cubic structure. We have determined their energy bands and densities of electronic states by means of the non-self-consistent augmented-plane-wave (APW) method. The results show that the nine hydrides are semiconductors with relatively large energy gaps. These isostructural and isoelectronic families of hydrides have been studied in order to establish correlations between the ordering of the electronic states and the energy gaps in terms of differences in metal–hydrogen distances and atomic energy levels. We observe that the splitting between the bonding and antibonding M' $d_{e_g}$ orbitals is responsible for the increase of the energy gap as the atomic number of M' increases. Nevertheless, the presence of d states from the divalent metals Ca and Sr modifies the nature of the unoccupied conduction states above the energy gaps. In general, a reduction of the energy gap is obtained in the Ca- and Sr-derived hydrides.

## 1. Introduction

The hydrides of general formula $M_2M'H_x$ involving divalent metals M, a transition metal M' (from families 8–10) and with hydrogen stoichiometry ranging from four to six crystallize in the fluorite ($Fm3m$) structure, also known as the $K_2PtCl_6$-like structure. The first intermetallic hydrides of this type were synthesized by Reilly and Wiswall (1968) and Moyer and co-wokers (1971). The system $Mg_2NiH_4$ has been extensively studied due to its reversible hydrogen absorption properties and to its potential technological applications. Excepting $Mg_2NiH_4$, the hydrides $M_2M'H_6$ (M=Mg, Ca, Sr, M'= Fe, Ru, Os) are all obtained by syntering the metallic powders at moderate temperatures (460–500 °C) under a high-pressure hydrogen atmosphere (70–130 bar) for several days (Huang etal 1991). In all these cases, the parent intermetallic compounds do not exist, so direct hydriding is impossible.

While the metallic framework forms a fluorite structure, the localization of the hydrogen (deuterium) atoms in the structure has been the subject of speculation. Recently, reliable neutron diffraction data established that the H atoms form an octahedral cage around the transition metal. The H atoms are localized close to $(\frac{1}{4}, 0, 0)$ positions. This is particulary true for the $M_2M'H_6$ hydrides (deuterides) (Huang *et al* 1991m, Didisheim *et al* 1984). For the $M_2M'H_5$ hydrides (M'= Co, Rh and Ir) a square pyramidal arrangement was determined (Zolliker *et al* 1985, Zhuang *et al* 1981). The case of $Mg_2NiH_4$ was more difficult to resolve owing to several possible geometries: square planar or tetrahedral in the low-temperature phase.

Regarding the hydrides of formula $M_2M'H_6$ (M=Mg, Ca, Sr, M'= Fe, Ru, Os), a systematic study concerning the synthesis and structural properties was recently published

0953-8984/93/366697+22$07.50  

(Huang *et al* 1991, Kritikos *et al* 1990). Among these hydrides, only three have been the subject of property characterization $Mg_2FeH_6$ (Didisheim *et al* 1984), $Ca_2RuH_6$ and $Sr_2RuH_6$ (Moyer *et al* 1971). In fact, reliable magnetic, electric and spectroscopic measurements are difficult to perform in these materials. Impurities are frequently present and the hydrides are obtained in powder form (while the former is the result of the synthesis conditions, the latter is inherent to these brittle materials).

Electric conductivity measurements (at room temperature) in compressed powder hydrides exist for $Ca_2RuH_6$ and $Sr_2RuH_6$. These materials show poor electrical conductivity ($\sim 10^{-7}$–$10^{-8}\ \Omega^{-1}\ cm^{-1}$). It seems that these materials are in general non-conducting.

Magnetic susceptibility measurements have been interpreted in terms of an Fe $d^6_{t_{2g}}$ diamagnetic low-spin complex $[Fe(II)H_6]^{4-}$ in $Mg_2FeH_6$. This conclusion is supported by Mössbauer, IR and Raman spectroscopies (Didisheim *et al* 1984). Nevertheless the weak paramagnetism observed could originate from the presence of free Fe in the samples as argued by the authors. The same kinds of argument have been put forward to interpret magnetic data of $Ca_2RuH_6$ and $Sr_2RuH_6$ hydrides which show also a weak paramagnetic ($Ca_2RuH_6$ and other $M_2M'H_5$ hydrides) or diamagnetic ($Sr_2RuH_6$) behavior (Moyer *et al* 1971).

Due to the large M′–M′ distances in these intermetallic hydrides compared to those in the M′ elemental solid and the short M′–H distances, a large ligand field splitting is expected. A common feature of the electronic structure of $Mg_2NiH_4$, $Mg_2CoH_5$ and $Mg_2FeH_6$ is the presence of a splitting between the bonding and antibonding M′ $d_{e_g}$ states (Gupta and Schlapbach 1988). The main features of the electronic structure of $Mg_2FeH_6$ will be summarized prior to presenting our results in the corresponding section. We only point out here that the electronic structure of $Mg_2NiH_4$, $Mg_2CoH_5$ and $Mg_2FeH_6$ show stabilization of the hydrogen bonding as the number of d electrons increases as well as the presence of a narrow M′ $d_{t_{2g}}$ band separated by a gap from the low-lying energy bands in the case of Fe- and Co-derived hydrides (Gupta 1984, Gupta *et al* 1984, Belin *et al* 1987, Orgaz and Gupta 1987).

Electron spectroscopies are in good agreement with theory. The calculations reproduce reasonably well the general characteristics of the occupied states as deduced by x-ray emission spectroscopy of the Ni L$\alpha$, Co L$\alpha$ and Mg K$\beta$ (Gupta *et al* 1984, Belin *et al* 1987). The experimental studies of x-ray absorption of Mg K and self-absorption of the Co L$\alpha$ in the $Mg_2CoH_5$ hydride confirm the presence of empty antibonding M′ d states above the Fermi level.

In the light of the newly synthesized and structurally characterized hydrides belonging to the $M_2M'H_6$ family (Huang *et al* 1991, Kritikos *et al* 1990), we have calculated, from first principles, the electronic band structure and density of electronic states of the $M_2M'H_6$ hydrides (M=Mg, Ca, Sr, M′= Fe, Ru, Os). Next, we discuss the trends in the values of the energy gaps and the ordering of the states in the series of compounds in terms of differences in crystallographic data and atomic energy levels. A preliminary account of this research was presented at the International Symposium on Metal–Hydrogen Systems (Orgaz and Gupta 1993).

## 2. Methodology

The electronic properties of the intermetallic hydrides $M_2M'H_6$ have been studied by means of the augmented-plane-wave (APW) method (Mattheiss *et al* 1968) in its non-self-consistent version using the X$\alpha$–Slater method (Slater 1951) ($\alpha = 1$) for the exchange term of the

potential. It is our experience, from previous investigations of several hydrides, that our results are very similar to those of self-consistent calculations performed with the von Barth–Hedin (1972) exchange potential in the local density approximation. Due to the short M'–H distance, the muffin-tin (MT) spheres leave more than 50% of the unit cell volume as an interstitial region. The departure of the potential outside the MT spheres from a constant value was taken into account (warped MT correction).

The energy eigenvalues and wave functions have been calculated *ab initio* at 89 points in the irreducible wedge of the Brillouin zone (IBZ) of the FCC structure. The base expansion of the APWs has been selected for each system in order to guarantee the convergence of the eigenvalues within 1 mRyd or less. The density of states (DOS) has been calculated by the linear energy tetrahedron method (Lehmann and Taut 1972) using 6048 tetrahedra in the IBZ. The *ab initio* energy bands were expanded into a set of 50 symmetrized plane waves giving a maximum RMS error of 2 mRyd. In table 1 we show the crystal parameters used in these calculations.

**Table 1.** Structural parameters (in Å) for $M_2M'H_6$.

| | | Fe | Ru | Os |
|---|---|---|---|---|
| Mg | a | 6.4300 [a] | 6.6294 [b] | 6.6822 [c] |
| | d(M-M') | 2.7843 | 2.8706 | 2.8900 |
| | d(M-H) | 2.2739 | 2.3439 | 2.3630 |
| | d(M'-H) | 1.5560 | 1.6734 | 1.6820 |
| | $V_{cell}$ | 265.85 | 291.36 | 298.37 |
| Ca | a | 7.0360[1,b] | 7.2290 [d] | 7.2361[2,b] |
| | d(M-M') | 3.0467 | 3.1302 | 3.1333 |
| | d(M-H) | 2.4916 | 2.5606 | 2.5596 |
| | d(M'-H) | 1.6180 | 1.6504 | 1.7280 |
| | $V_{cell}$ | 348.32 | 377.78 | 378.89 |
| Sr | a | 7.3170 [b] | 7.6000 [e] | 7.6260 [b] |
| | d(M-M') | 3.1684 | 3.2900 | 3.3022 |
| | d(M-H) | 2.5901 | 2.6900 | 2.7013 |
| | d(M'-H) | 1.7012 | 1.6900 | 1.7410 |
| | $V_{cell}$ | 391.74 | 438.98 | 443.50 |

1 data of $Ca_{1.98}Mg_{0.02}FeD_6$
2 data of $Ca_{1.92}Mg_{0.08}OsD_6$
a [Didisheim 1984]
b [Huang 1991]
c [Kritikos 1990]
d [Lindsay 1989]
e [Moyer 1971]

## 3. Results and Discussion

The electronic structure of the nine intermetallic hydrides is displayed in figures 1, 2 and 3. The energy bands along the high symmetry directions of the FCC Brillouin zone and the partial wave analysis of the DOS at each atomic site are shown for selected hydrides. The total DOSs for the nine hydrides are plotted in figure 2. The low-energy structure (below the Fermi energy) contains 18 electrons corresponding to nine filled bands per unit cell. In table 2 we report the band widths and energy gaps for the nine calculated hydrides. From a quick inspection of the energy bands (figure 1) and total DOSs of these hydrides

**Table 2.** Band widths and energy gaps (in eV). $\omega_l$ represents the band width of each structure in the DOS plot in increasing energy order, $\Delta_l$ is the intermediate energy gap between these structures and, $\Delta_g$ is the energy gap between the valence and conduction band.

| | $Mg_2FeH_6$ | $Mg_2RuH_6$ | $Mg_2OsH_6$ |
|---|---|---|---|
| $\omega_1$ | 7.23 | 7.19 | 7.07 |
| $\Delta_1$ | 1.17 | — | — |
| $\omega_2$ | 1.25 | — | — |
| $\Delta_g$ | 1.74 | 3.51 | 4.01 |

| | $Ca_2FeH_6$ | $Ca_2RuH_6$ | $Ca_2OsH_6$ |
|---|---|---|---|
| $\omega_1$ | 1.55 | 2.18 | 1.76 |
| $\Delta_1$ | 1.33 | 0.40 | 0.90 |
| $\omega_2$ | 1.99 | 2.15 | 2.18 |
| $\Delta_2$ | 2.67 | 0.53 | 0.38 |
| $\omega_3$ | 0.63 | 0.46 | 0.50 |
| $\Delta_g$ | 1.58 | 2.84 | 3.29 |

| | $Sr_2FeH_6$ | $Sr_2RuH_6$ | $Sr_2OsH_6$ |
|---|---|---|---|
| $\omega_1$ | 1.48 | 1.35 | 1.23 |
| $\Delta_1$ | 1.27 | 1.47 | 1.54 |
| $\omega_2$ | 1.61 | 1.25 | 1.35 |
| $\Delta_2$ | 2.87 | 0.93 | 0.73 |
| $\omega_3$ | 0.50 | 0.30 | 0.33 |
| $\Delta_g$ | 1.31 | 3.27 | 3.46 |

(figure 2) some general features can be drawn. As indicated in section 1, we found these nine compounds to be semiconductors with relatively large energy gaps (see table 2).

The important role played by the $M'H_6$ octahedral complex in determining the electronic properties of these intermetallic hydrides has been pointed out in section 1 (Gupta 1984, Orgaz and Gupta 1987, Gupta and Schlapbach 1988). The direct interactions between the octahedral $M'H_6$ cages are rather weak due to the large distances between them. These interactions are mediated via the cubic array formed by the divalent element.

As an example, we summarize the results of the band structure calculation of $Mg_2FeH_6$. In figures 1(a), 2(a) and 3(a) we show the energy bands, total DOS and partial wave analysis of the DOS for $Mg_2FeH_6$. In increasing order of energy at the Brillouin zone centre $\Gamma$ point, we observe (figure 4(a) and table 3), (i) the $\Gamma_1$ state corresponding to an Mg s/Fe s hybridized state lowered in energy by H s interactions, (ii) a doubly degenerate $\Gamma_{12}$ state resulting from the bonding interaction between the Fe $d_{e_g}$ and H s states (the lobes of these d states point towards the hydrogen sites), and (iii) a triply degenerate H s state hybridized with the Fe p states. These six low-energy bands are separated from the next three occupied bands formed by the almost pure Fe $d_{t_{2g}}$ states which do not interact with the H atoms. The total DOS (figure 2(a)) and their partial wave analysis around each atomic site show a low-energy structure due to the Fe–H and H–H interactions and a weak Mg s and p hybridization. The band width of this structure, $\omega_1$, is 7.23 eV. A second narrow structure ($\omega_2 = 1.25$ eV) in the DOS of the occupied states corresponds to the Fe $d_{t_{2g}}$ bands. The nine low-energy bands are filled by 18 electrons. The occupied non-bonding Fe $d_{t_{2g}}$ states are separated by an indirect energy gap ($\Delta_g = 1.74$ eV) between $\Gamma$ and X from the empty antibonding Fe $d_{e_g}$/H s states.

In order to understand the role of the H atoms in the electronic properties of these

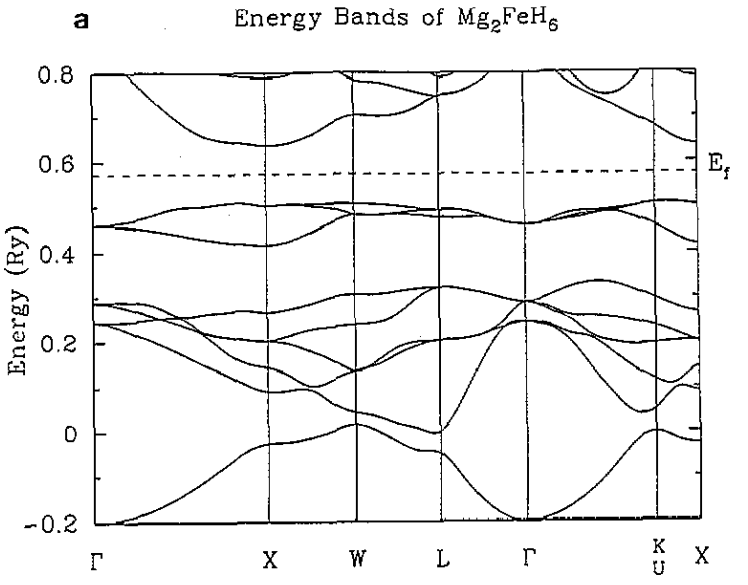


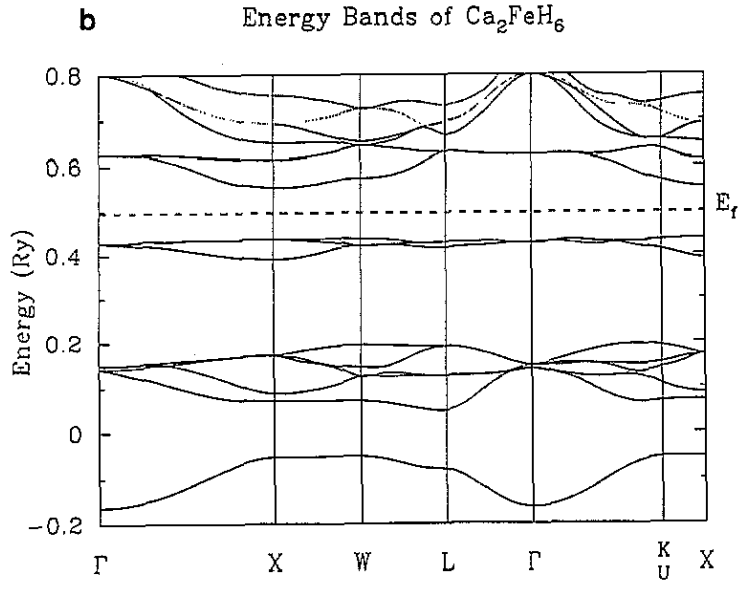


**Figure 1.** Energy-band diagrams of (a) $Mg_2FeH_6$, (b) $Ca_2FeH_6$, (c) $Sr_2FeH_6$, (d) $Ca_2RuH_6$ and (e) $Ca_2OsH_6$.

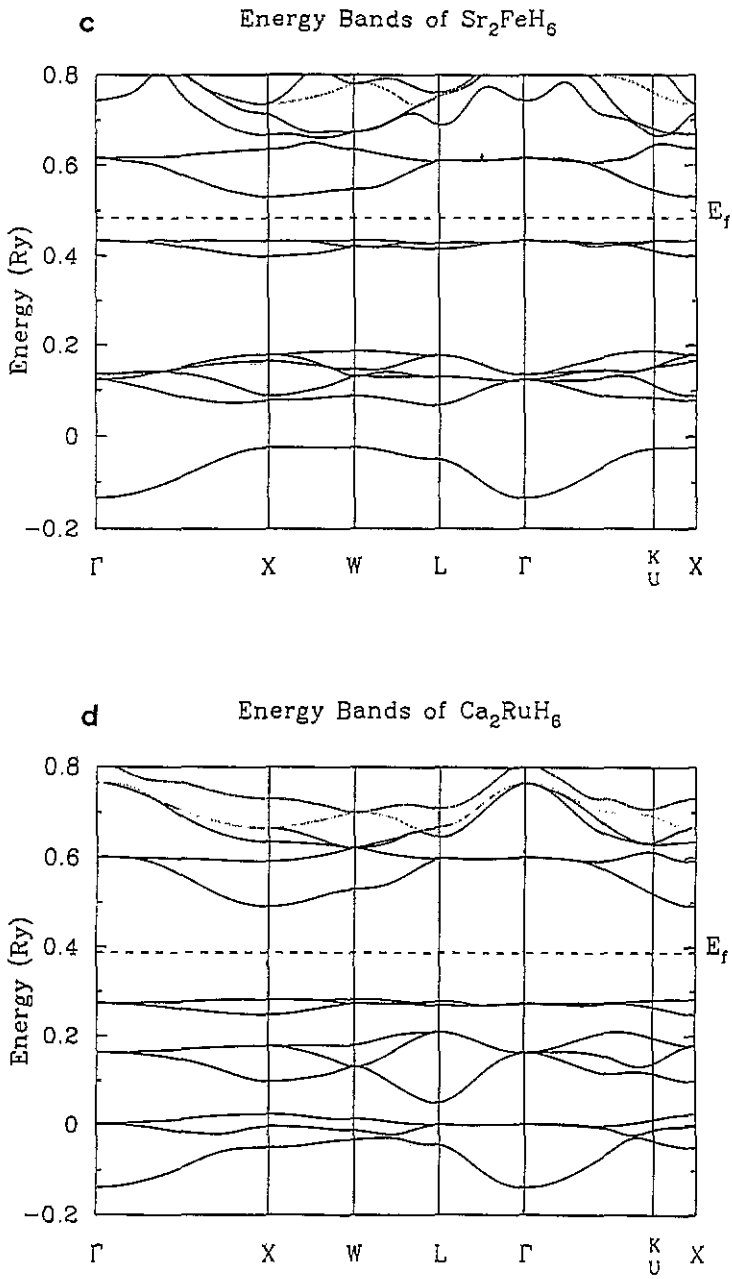


**Figure 1.** (Continued)

intermetallic hydrides, we calculated the energy eigenvalues at the Γ point of $Mg_2FeH_0$ and $Ca_2FeH_0$. These calculations were performed by using the MT potential of the hydride but without considering the H atoms in the secular equation elements. We also calculated

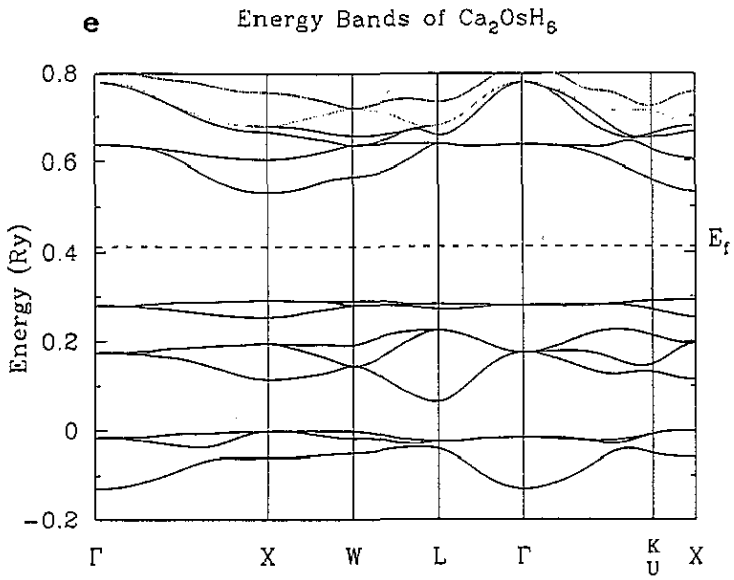


**Figure 1.** (Continued)

the energy eigenvalues at the Γ point for the fictitious intermetallic systems $M_2M'$. Some numerical differences are present between the calculations ($M_2M'H_0$ versus $M_2M'$ systems) but the character and ordering of the eigenstates remain the same. These results are to be compared with those of $Mg_2FeH_6$ and $Ca_2FeH_6$. In figure 4 we show the energy eigenvalues at the Γ point for $Mg_2FeH_0$ and $Mg_2FeH_6$, and $Ca_2FeH_0$ and $Ca_2FeH_6$. In both calculations, with and without H, the crystal parameters remain unchanged, so we observe only the effect of the H atoms on the metallic energy levels. In figure 4(a) we observe that the presence of H atoms in the structure results in the hybridization of the H s/Mg s/Fe s states which are lowered in energy at the bottom of the energy scale. A stabilization of the Fe $d_{e_g}$ manifold is observed due to the bonding interaction with the H s states. This leads to a drastic increase of the crystal field splitting between the bonding d-$e_g$/H s states and the d-$t_{2g}$ non bonding states. The antibonding counterpart of the Fe $d_{e_g}$/H s states appears in the conduction bands. Finally the Fe $d_{t_{2g}}$ states observe a slight decrease in energy and the new triply degenerate H s hydride states are now present slightly hybridized with the Fe p states.

The case of $Ca_2FeH_x$ is more complicated owing to the presence of the Ca d states. It is important to note that the main part of the Ca d contribution appears above the Fermi level in all the compounds studied. In the H-free system $Ca_2FeH_0$ (figure 4(b)), in addition to the pure Ca d states, hybridized Fe d/Ca d states are present just above the occupied bands. These new hybrid states are responsible for the reduction in the energy-gap value observed in the Ca- and Sr-based hydrides.

We consider now only the effect of the transition metal in the $Mg_2M'H_6$ hydrides (M'= Fe, Ru, Os). It is important to note that the cell volume and M'–H distance increase, as shown in table 1, as the atomic number of M' increases. At the same time, the spatial extention of the d orbitals increases from the 3d to the 4d and 5d element. The trend observed in this series is an increase in the energy splitting between the filled bonding M' $d_{e_g}$/H s states and their empty antibonding counterparts as the atomic number of M' increases. This shows that the covalent bonding between the transition metal d-$e_g$ and H s states becomes stronger. The greater overlap between M' $d_{e_g}$ and H s states, as the atomic

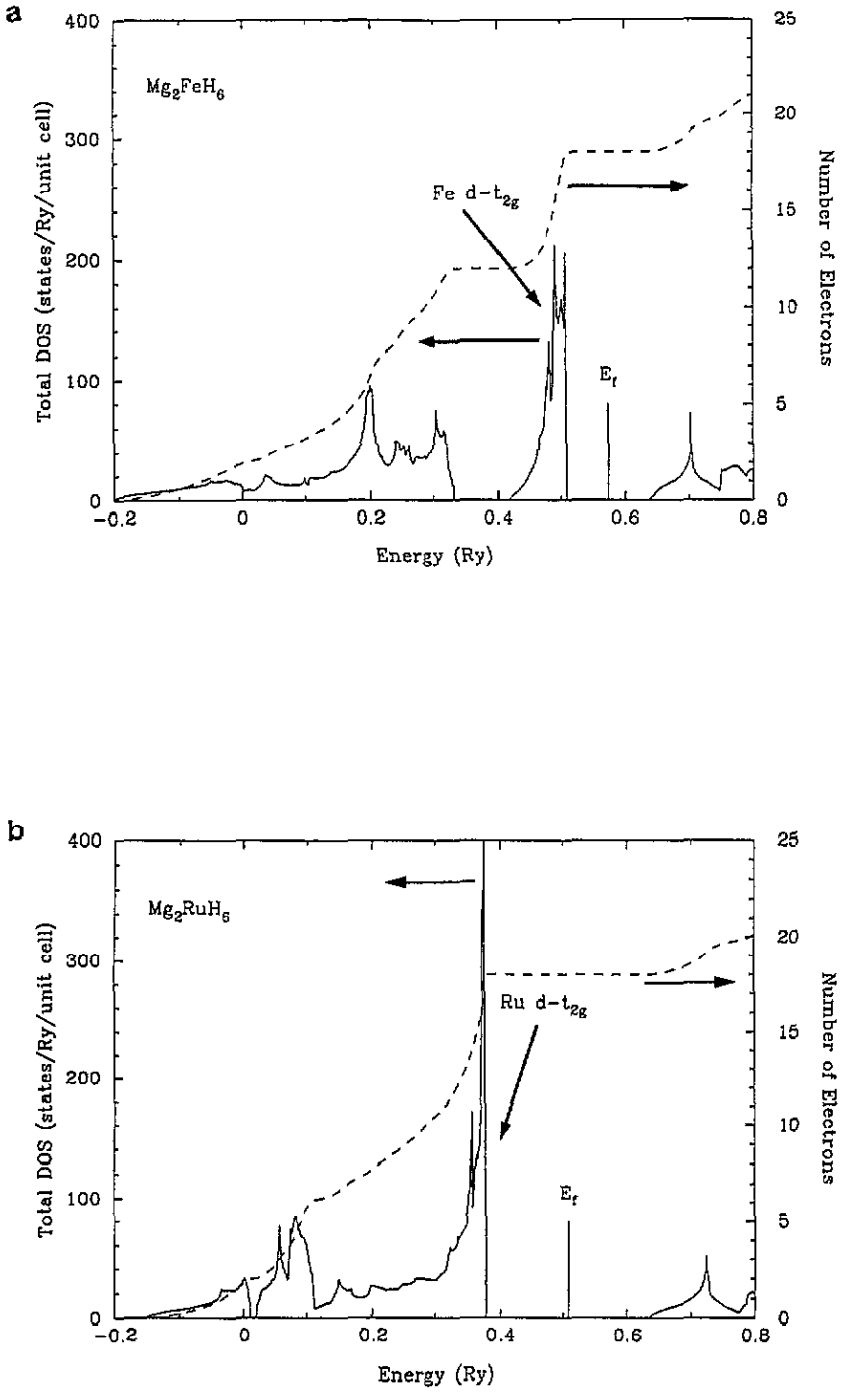


**Figure 2.** Total DOS (states $Ryd^{-1}$/unit cell) of (a) $Mg_2FeH_6$, (b) $Mg_2RuH_6$, (c) $Mg_2OsH_6$, (d) $Ca_2FeH_6$, (e) $Ca_2RuH_6$, (f) $Ca_2OsH_6$, (g) $Sr_2FeH_6$, (h) $Sr_2RuH_6$ and (i) $Sr_2OsH_6$.

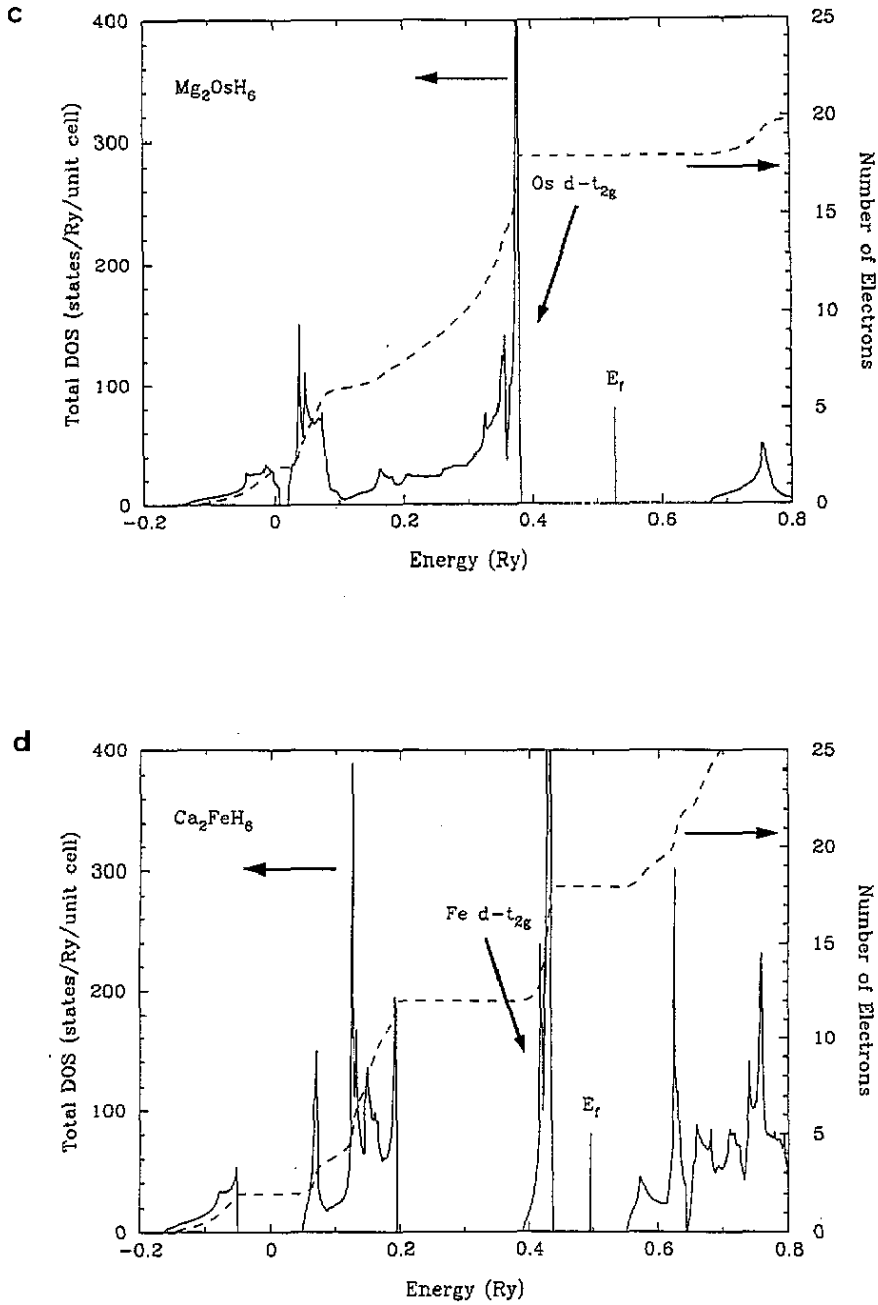


**Figure 2.** (Continued)

number of M′ increases, is due to the larger delocalization of the 5d compared to 4d and 3d orbitals which overcomes the effect of the concomitant increase in the M′–H distances, the latter adversely affects the orbital overlap and covalent bonding strength. Since the splitting

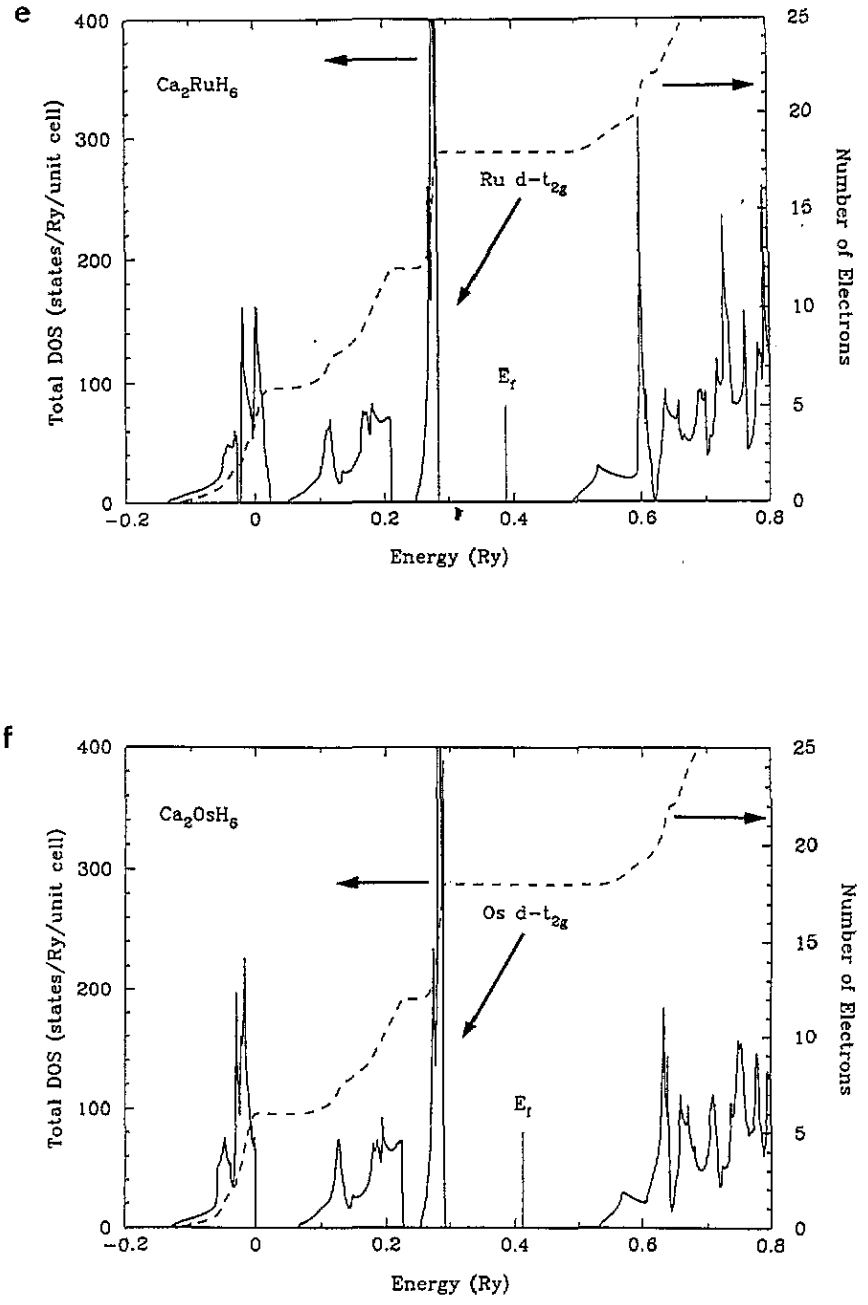


**Figure 2.** (Continued)

between the occupied M′ $d_{t_{2g}}$ and M′ $d_{e_g}$ states remains essentially constant in the series while the antibonding empty M′ $d_{e_g}$ states are destabilized, the overall effect in the DOS (figure 2(a–c)) is to produce a larger energy gap $\Delta_g$ in going from Fe ($\Delta_g$ = 1.74 eV) to

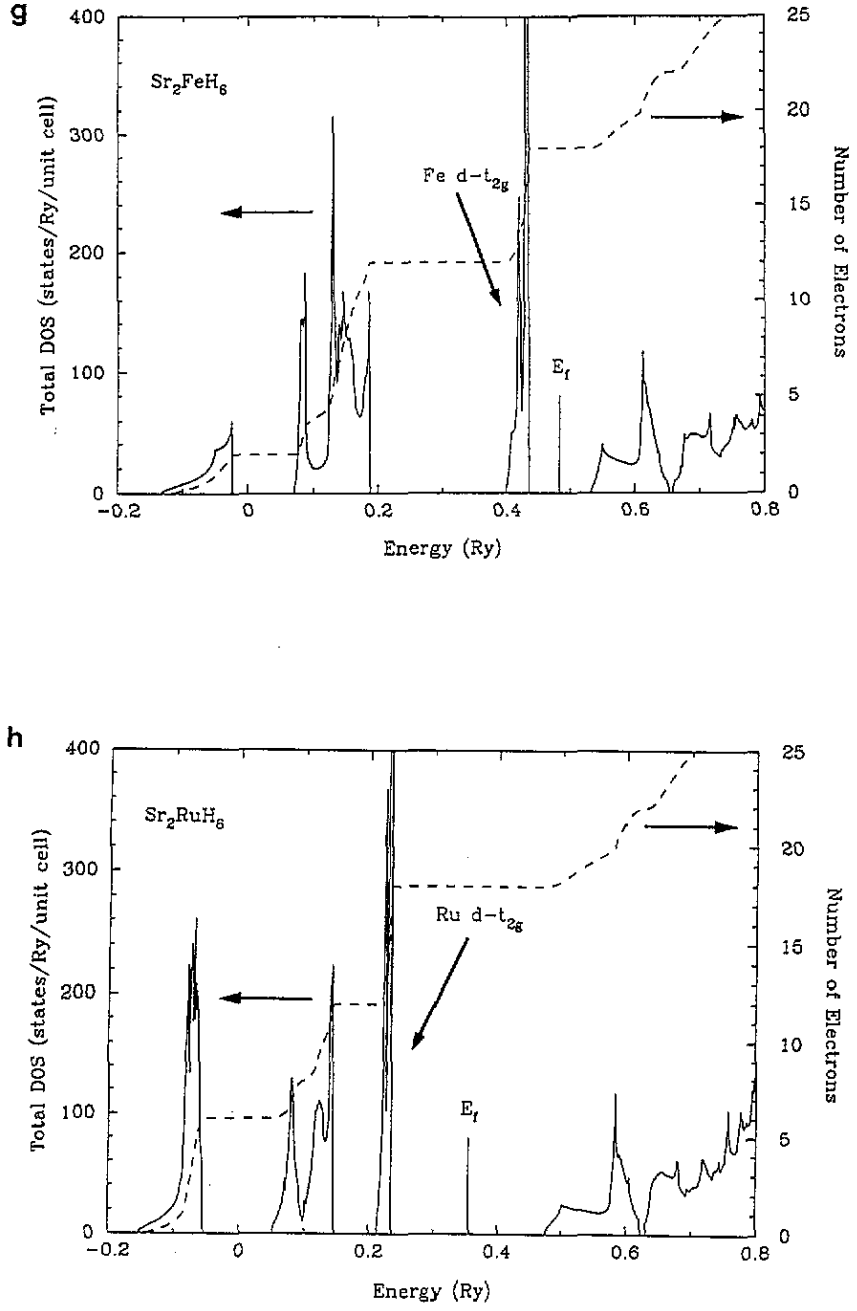


**Figure 2.** (Continued)

Ru ($\Delta_g$ = 3.51 eV) and Os ($\Delta_g$ = 4.01 eV) (see table 2).

In this series, the stabilization of the M' $d_{t_{2g}}$ manifold and the slight energy increase in the pure H s states at Γ (see figure 5(a)) results in a merging of the two structures which

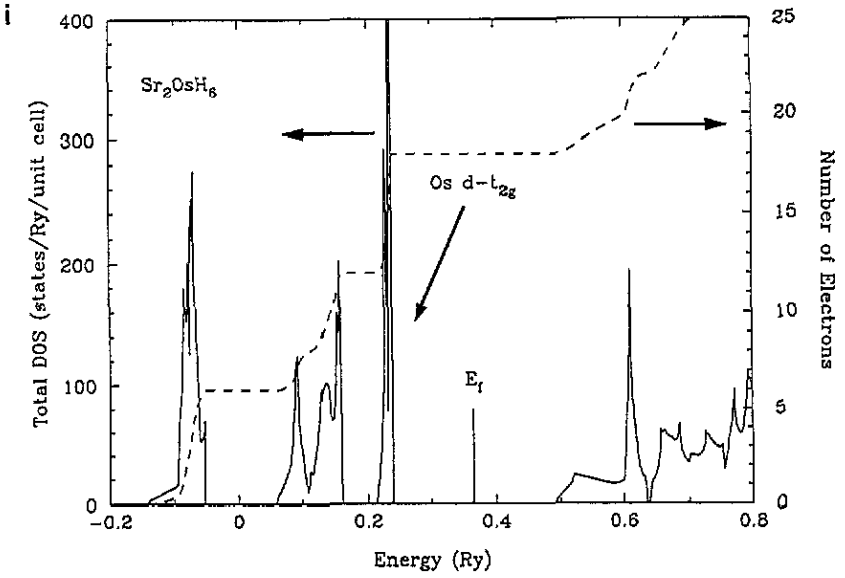


**Figure 2.** (Continued)

produce a sole large complex structure of width $\omega_1$ in $Mg_2RuH_6$ and $Mg_2OsH_6$ as shown in table 2 and figure 2(b, c).

The series containing the same transition metal (M′=Fe) but Mg, Ca or Sr as divalent metal shows a different behaviour. In figures 1(a–c), 2(a, d, g) and 3(a–c) we show the energy bands, total DOS and the partial wave analysis of the DOS at each atomic site for these hydrides. In tables 3 and 4, we show the wave function analysis at the Γ and X points at the different atomic sites for the first 12 bands, for $Mg_2FeH_6$ and $Ca_2FeH_6$, respectively. Note that the cell volume and the M′–H distance increase with the atomic number of M. In the $M_2FeH_6$ series the position of the $\Gamma_1$ H s/M s/Fe s state increases in energy relative to the bottom of the transition metal d states. This is due to the decrease in the transition metal s electrons compression accompanying the lattice expansion. In contrast to the Mg series, the $t_{2g}$ states remain at essentially the same energy since these states are non bonding and the transition metal (Fe) is unchanged. The splitting between the bonding Fe $d_{e_g}$/H s and the Fe $d_{t_{2g}}$ states increases slightly in this series from Mg to Ca and Sr in spite of the increase in the Fe–H distances due to the additional although weak bonding component with the Ca(Sr) d states.

The triply degenerate H s states now show some hybridization with the Ca(Sr) d orbitals and are lowered in energy. This leads to a different ordering of the bonding states at Γ in the compound $Sr_2FeH_6$. This can be clearly seen in the energy bands and DOS plots. A complex structure ($\omega_2$) involving the Fe $d_{e_g}$ and the H s states slightly hybridized with Ca(Sr) d states is well separated from the low-energy metals/H s structure and from the narrow Fe $d_{t_{2g}}$ structure. An important feature is the presence, at the bottom of the conduction band, of new Ca(Sr) d/Fe d antibonding states which are responsible for the reduction of the energy gap, as was previously mentioned (see table 2). The divalent metal d component at the bottom of the conduction band is particularly important in the case of Ca.

In the $Ca_2M'H_6$ series we observe the effect of M′ (Fe, Ru, Os) when Ca d states are present. In figure 1(b, d, e), 2(d–f) and 3(b, d, e) we show the energy bands, total DOS and the partial wave analysis of the DOS for the Ca-derived hydrides. In figure 5(c) the

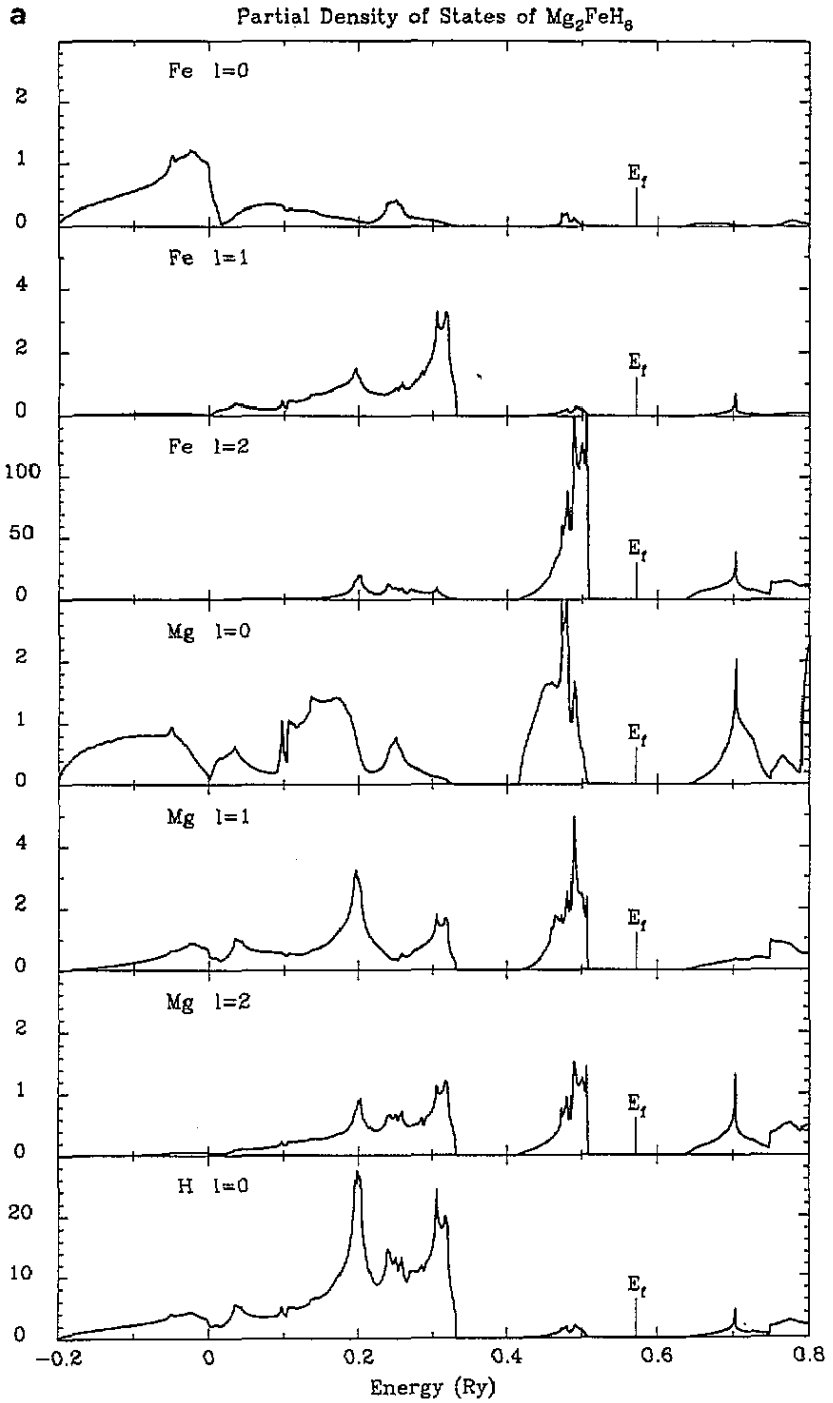


**Figure 3.** Partial wave analysis of the DOS (states $Ryd^{-1}$/unit cell) for each atomic site of (a) $Mg_2FeH_6$, (b) $Ca_2FeH_6$, (c) $Sr_2FeH_6$, (d) $Ca_2RuH_6$ and (e) $Ca_2OsH_6$.

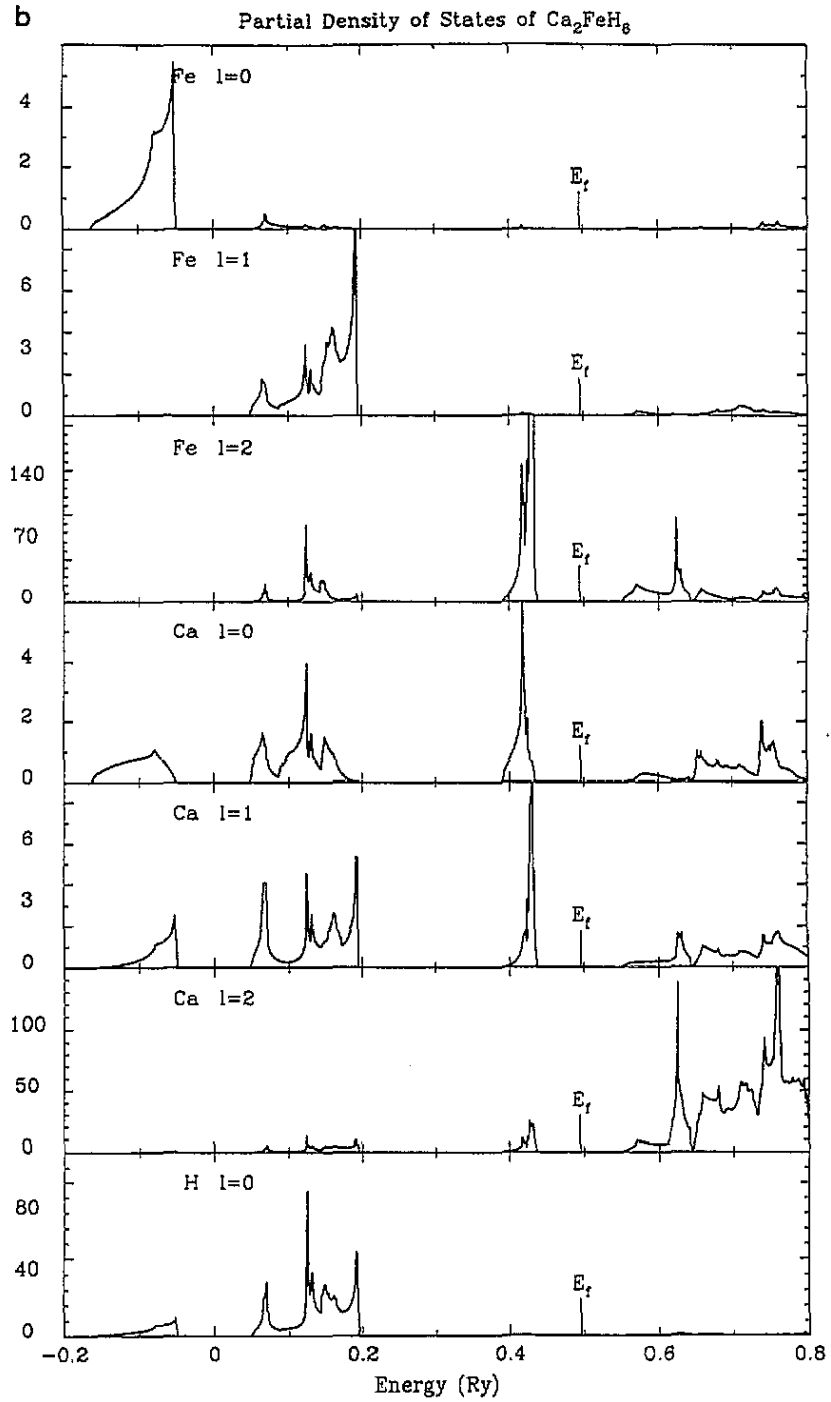


**Figure 3.** (Continued)

energy eigenvalues are plotted at the Γ point. The wave function analysis is summarized in tables 4, 5 and 6. Again, the increase of the energy gap (now between the filled M′ $d_{t_{2g}}$ and empty M′ d/Ca d states) is mainly due to the increase in the atomic charge of M′

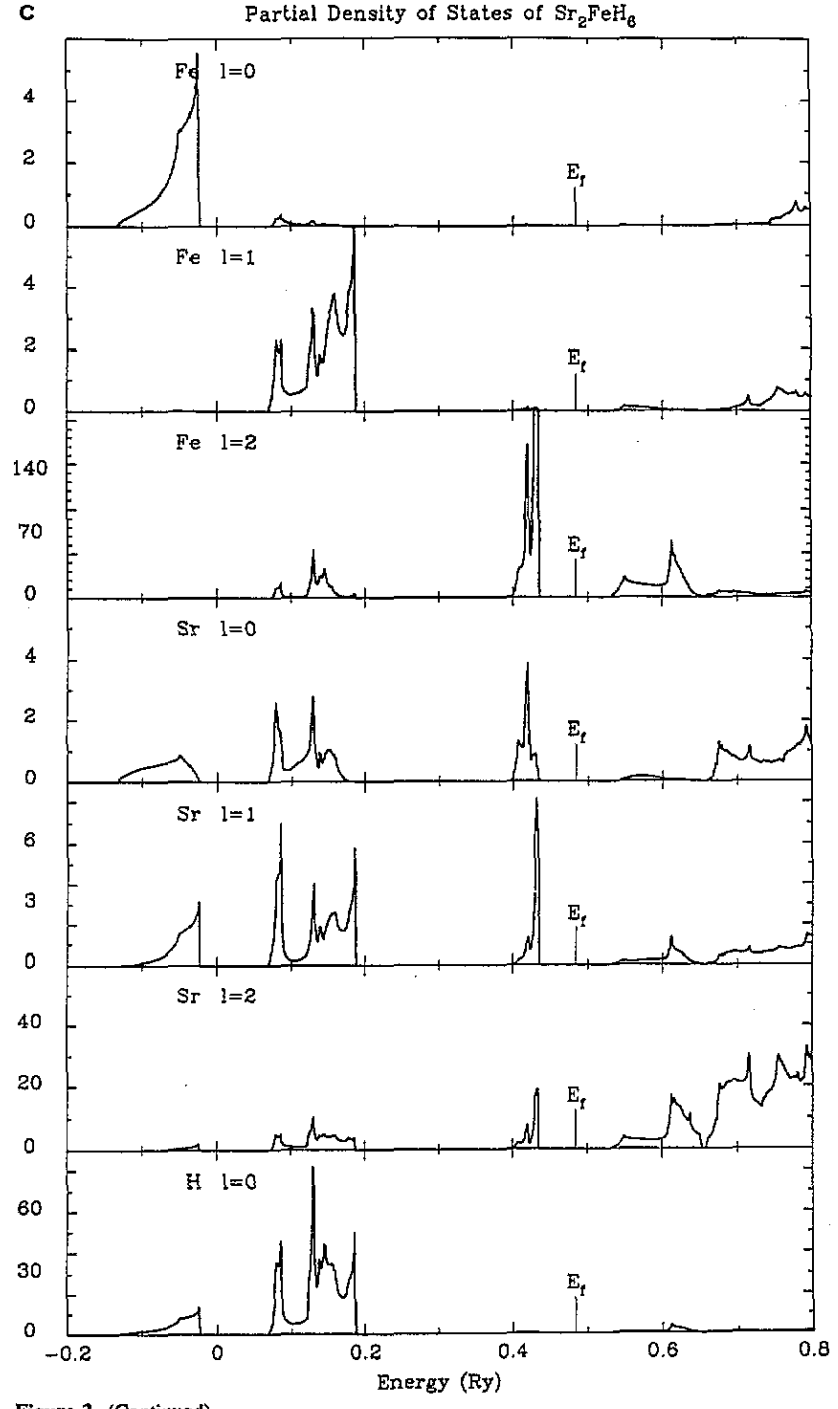


**Figure 3.** (Continued)

while the M′ d/Ca d states remain at essentially the same energy. In this series, the complex structure $\omega_2$, M′ $d_{e_g}$/H s splits from the Ca d/H s states in the $Ca_2RuH_6$ and $Ca_2OsH_6$ cases, as appears clearly in the DOS plot (figure 2(d–f)). The states merge with the metals/H s

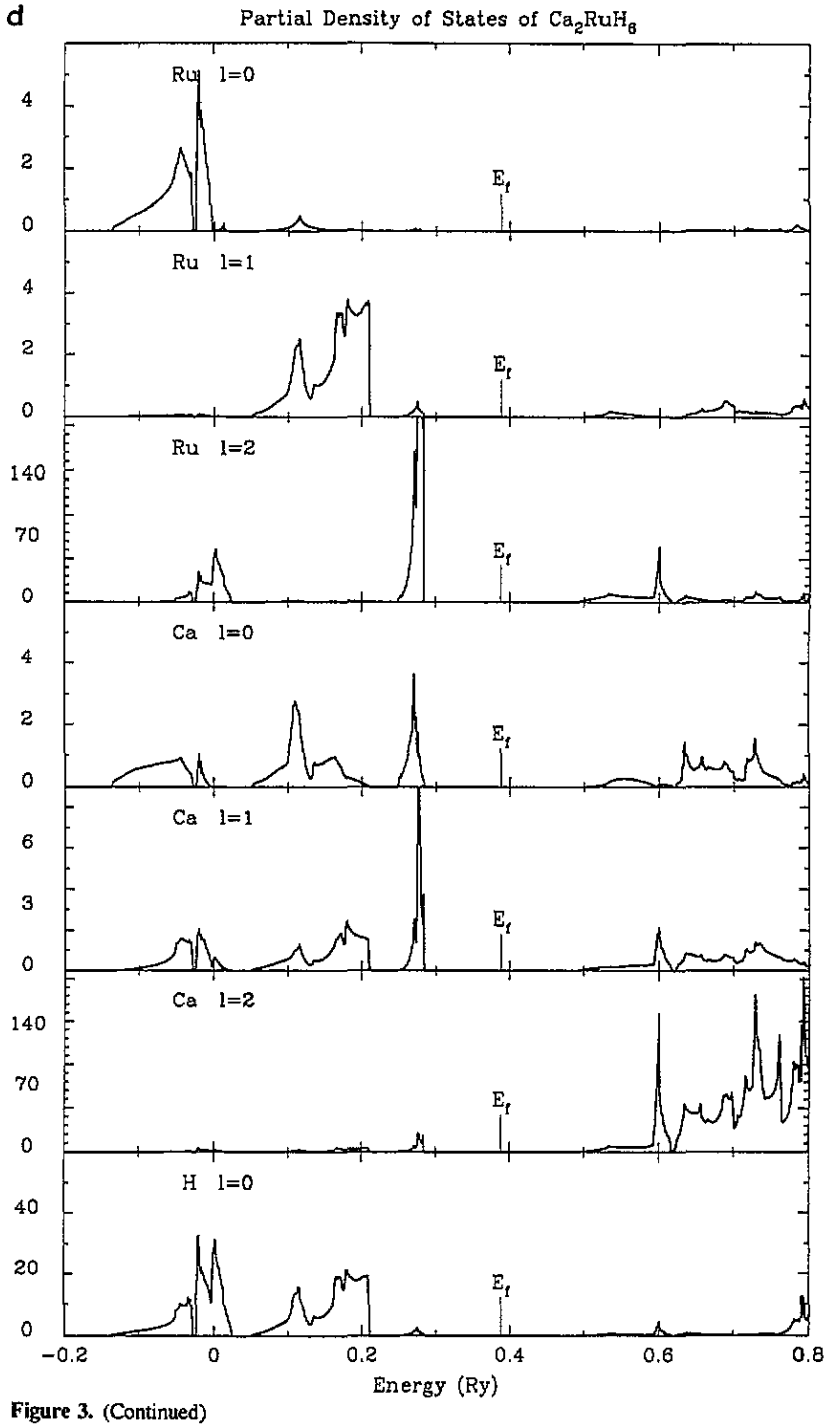


**Figure 3.** (Continued)

low-energy band as the atomic number of M′ increases.

The low-energy metals/H s band merges with the bonding M′ $d_{e_g}$/H s states for M′ = Ru and Os. This is essentially due to the decrease in the compression of the metal s electrons

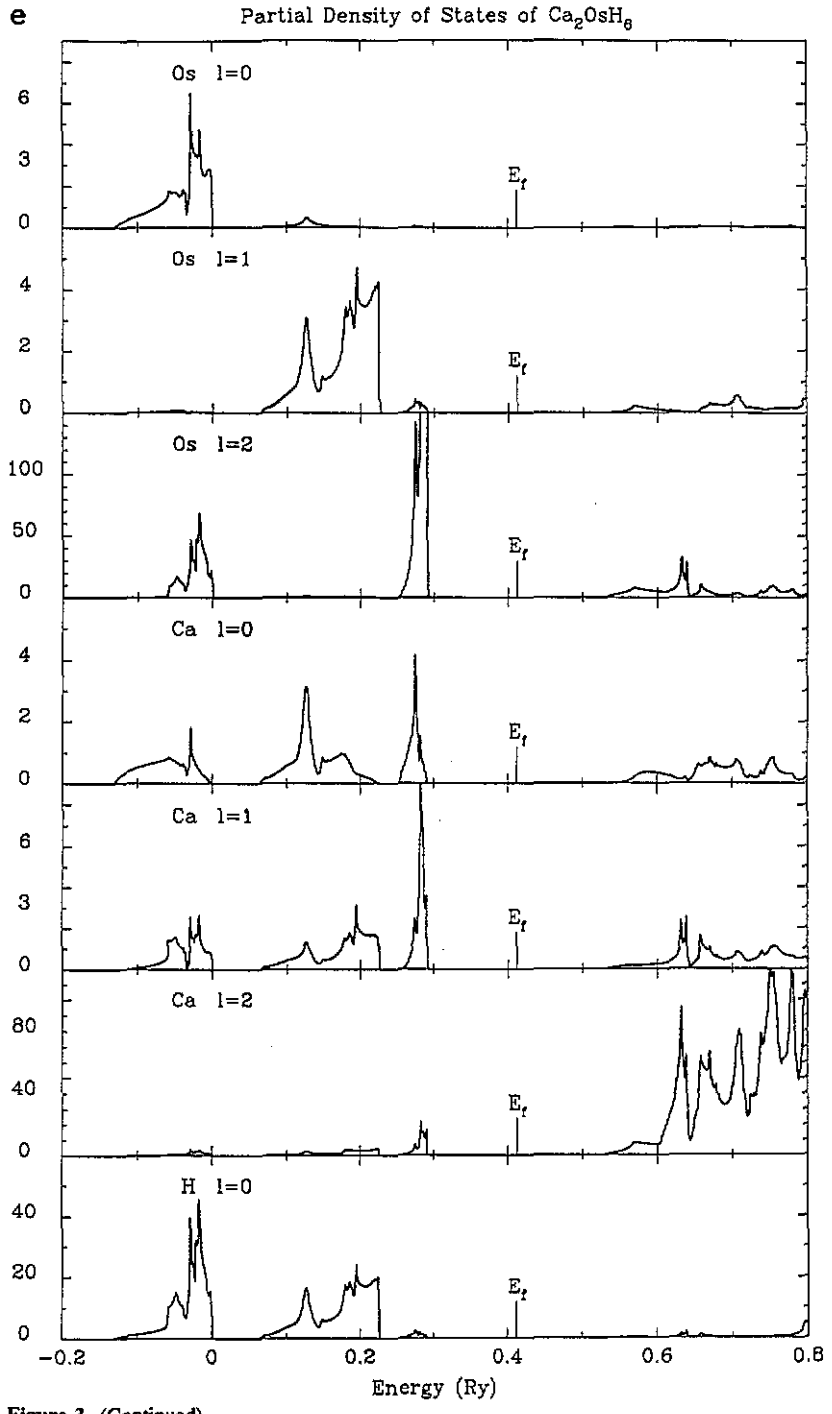


**Figure 3.** (Continued)

with the lattice expansion when the atomic charge of M′ increases. In the series $Sr_2M'H_6$ (M′ = Fe, Ru, Os) the ordering of the electronic states can be discussed directly from the DOS plots (figure 2(g–i)). In $Sr_2FeH_6$, the complex structure of width $\omega_2$, which is composed

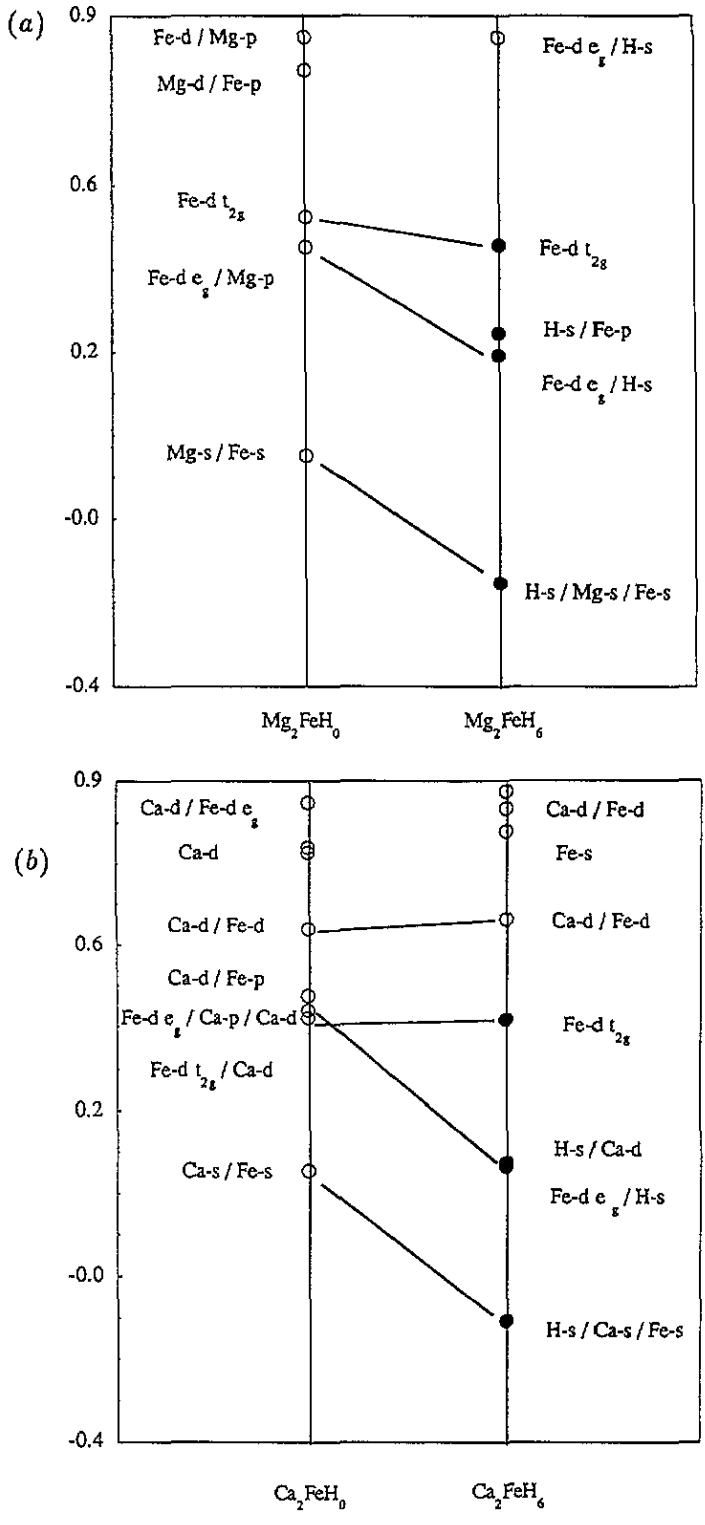


**Figure 4.** Energy diagram of the Γ-point eigenvalues (Ryd) for (filled circles represent occupied states) (a) $Mg_2FeH_6$ and $Mg_2FeH_0$ and (b) $Ca_2FeH_6$ and $Ca_2FeH_0$.

**Table 3.** Wave function analysis for $Mg_2FeH_6$ at the Γ and X points for the first 12 bands.

| Bands | Degeneracy | E (Ry) | Fe s | Fe p | Fe d | Mg s | Mg p | H s |
|---|---|---|---|---|---|---|---|---|
| 1 | 1 | -.201 | .06 | .00 | .00 | .12 | .00 | .22 |
| 2,3 | 2 | .244 | .00 | .00 | .38 | .00 | .00 | .27 |
| 4,5,6 | 3 | .288 | .00 | .05 | .00 | .00 | .00 | .38 |
| 7,8,9 | 3 | .460 | .00 | .00 | .62 | .00 | .07 | .00 |
| 10,11 | 2 | .859 | .00 | .00 | .56 | .00 | .00 | .16 |
| 12 | 1 | .902 | .00 | .00 | .29 | .00 | .24 | .00 |

| Bands | Degeneracy | E (Ry) | Fe s | Fe p | Fe d | Mg s | Mg p | H s |
|---|---|---|---|---|---|---|---|---|
| 1 | 1 | -.026 | .06 | .00 | .03 | .00 | .07 | .26 |
| 2 | 1 | .091 | .00 | .04 | .00 | .14 | .00 | .23 |
| 3 | 1 | .143 | .05 | .00 | .15 | .00 | .00 | .30 |
| 4,5 | 2 | .202 | .00 | .05 | .00 | .00 | .08 | .30 |
| 6 | 1 | .266 | .00 | .00 | .43 | .00 | .00 | .27 |
| 7 | 1 | .416 | .00 | .00 | .48 | .14 | .00 | .00 |
| 8,9 | 2 | .502 | .00 | .00 | .80 | .00 | .01 | .00 |
| 10 | 1 | .637 | .01 | .00 | .66 | .00 | .01 | .02 |
| 11 | 1 | .790 | .00 | .00 | .43 | .25 | .00 | .00 |
| 12 | 1 | .892 | .00 | .00 | .52 | .00 | .00 | .25 |

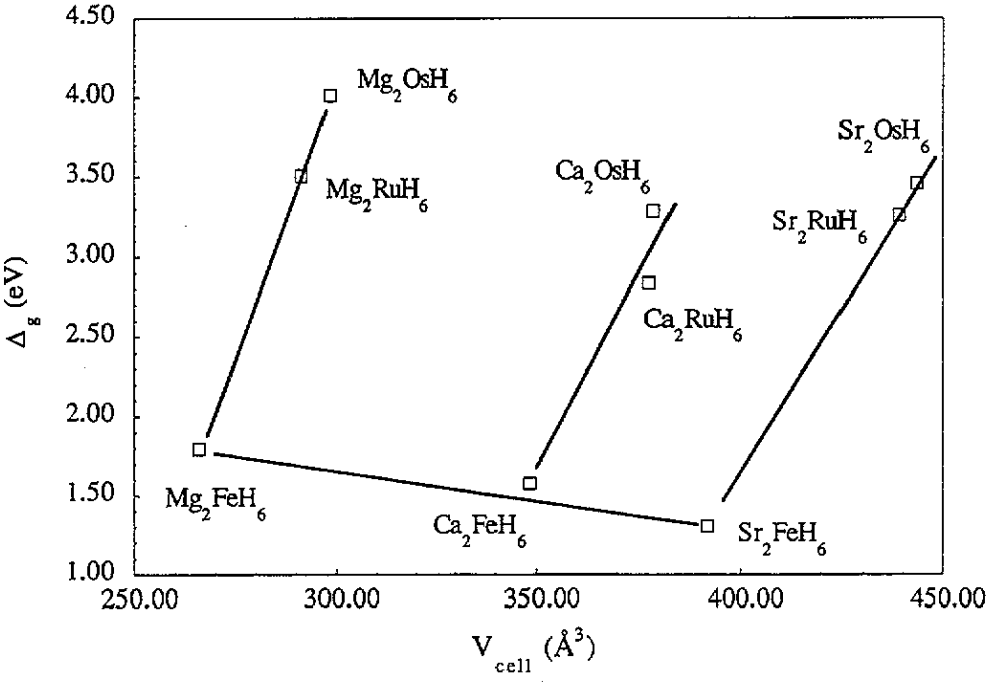


**Figure 5.** Correlation between the energy gap $\Delta_g$ (eV) and the unit cell volume (Å$^3$).

of M′ $d_{e_g}$/H s and H s states slightly hybridized with Sr d states, splits in the late members of the series (M′ = Ru, Os). For $Sr_2RuH_6$ and $Sr_2OsH_6$, the low-energy band merges with

**Table 4.** Wave function analysis for $Ca_2FeH_6$ at the Γ and X points for the first 12 bands.

| Bands | Degeneracy | E (Ry) | Fe s | Fe p | Fe d | Ca s | Ca p | Ca d | H s |
|---|---|---|---|---|---|---|---|---|---|
| 1 | 1 | -.162 | .07 | .00 | .00 | .09 | .00 | .00 | .20 |
| 2,3 | 2 | .141 | .00 | .00 | .30 | .00 | .00 | .06 | .23 |
| 4,5,6 | 3 | .149 | .00 | .05 | .00 | .00 | .00 | .12 | .27 |
| 7,8,9 | 3 | .427 | .00 | .00 | .71 | .00 | .03 | .02 | .00 |
| 10,11 | 2 | .625 | .00 | .00 | .36 | .00 | .00 | .45 | .00 |
| 12 | 1 | .801 | .13 | .00 | .00 | .04 | .00 | .00 | .01 |

| Bands | Degeneracy | E (Ry) | Fe s | Fe p | Fe d | Ca s | Ca p | Ca d | H s |
|---|---|---|---|---|---|---|---|---|---|
| 1 | 1 | -.052 | .10 | .00 | .00 | .00 | .05 | .02 | .23 |
| 2 | 1 | .072 | .00 | .00 | .19 | .00 | .01 | .05 | .24 |
| 3 | 1 | .088 | .00 | .04 | .00 | .09 | .00 | .04 | .22 |
| 4,5,6 | 3 | .172 | .00 | .05 | .00 | .00 | .06 | .00 | .28 |
| 7 | 1 | .390 | .00 | .00 | .55 | .06 | .00 | .07 | .00 |
| 8,9 | 2 | .436 | .00 | .00 | .72 | .00 | .01 | .06 | .00 |
| 10 | 1 | .553 | .00 | .00 | .56 | .00 | .01 | .12 | .00 |
| 11 | 1 | .614 | .00 | .00 | .00 | .00 | .00 | .72 | .00 |
| 12 | 1 | .651 | .00 | .00 | .27 | .05 | .00 | .46 | .00 |

**Table 5.** Wave function analysis for $Ca_2RuH_6$ at the Γ and X points for the first 12 bands.

| Bands | Degeneracy | E (Ry) | Ru s | Ru p | Ru d | Ca s | Ca p | Ca d | H s |
|---|---|---|---|---|---|---|---|---|---|
| 1 | 1 | -.137 | .07 | .00 | .00 | .09 | .00 | .00 | .19 |
| 2,3 | 2 | .002 | .00 | .00 | .39 | .00 | .00 | .03 | .19 |
| 4,5,6 | 3 | .163 | .00 | .04 | .00 | .00 | .00 | .11 | .26 |
| 7,8,9 | 3 | .274 | .00 | .00 | .68 | .00 | .03 | .01 | .00 |
| 10,11 | 2 | .602 | .00 | .00 | .24 | .00 | .00 | .52 | .01 |
| 12 | 1 | .766 | .00 | .00 | .01 | .00 | .01 | .89 | .00 |

| Bands | Degeneracy | E (Ry) | Ru s | Ru p | Ru d | Ca s | Ca p | Ca d | H s |
|---|---|---|---|---|---|---|---|---|---|
| 1 | 1 | -.050 | .01 | .00 | .24 | .00 | .03 | .00 | .20 |
| 2 | 1 | -.004 | .08 | .00 | .07 | .00 | .02 | .05 | .21 |
| 3 | 1 | .024 | .00 | .00 | .42 | .00 | .00 | .00 | .19 |
| 4 | 1 | .099 | .00 | .04 | .00 | .08 | .00 | .03 | .21 |
| 5,6 | 2 | .178 | .00 | .05 | .00 | .00 | .05 | .00 | .27 |
| 7 | 1 | .249 | .00 | .00 | .61 | .04 | .00 | .03 | .00 |
| 8,9 | 2 | .282 | .00 | .00 | .70 | .00 | .01 | .04 | .00 |
| 10 | 1 | .492 | .00 | .00 | .41 | .00 | .01 | .14 | .02 |
| 11 | 1 | .593 | .00 | .00 | .00 | .00 | .00 | .70 | .00 |
| 12 | 1 | .635 | .00 | .00 | .16 | .05 | .00 | .53 | .00 |

the two M′ $d_{e_g}$/H s bonding bands. Similar behaviour is observed in the $Ca_2M'H_6$ series for M′ = Ru and Os. The energy gap $\Delta_g$ increases as the atomic number of M′ increases, as in the case of the Ca series, due to the presence of the almost constant energy M′ d/Sr d states above the Fermi level and the stabilization of the M′ $d_{t_{2g}}$ states.

In all the compounds considered the energy gap is indirect. It appears between the top of the Γ–X direction and the bottom of the conduction band at X. In figure 5 we show the

**Table 6.** Wave function analysis for $Ca_2OsH_6$ at the Γ and X points for the first 12 bands.

| Bands | Degeneracy | E (Ry) | Os s | Os p | Os d | Ca s | Ca p | Ca d | H s |
|---|---|---|---|---|---|---|---|---|---|
| 1 | 1 | -.130 | .08 | .00 | .00 | .09 | .00 | .00 | .18 |
| 2,3 | 2 | -.015 | .00 | .00 | .38 | .00 | .00 | .03 | .19 |
| 4,5,6 | 3 | .176 | .00 | .05 | .00 | .00 | .00 | .11 | .26 |
| 7,8,9 | 3 | .280 | .00 | .00 | .64 | .00 | .03 | .01 | .00 |
| 10,11 | 2 | .637 | .00 | .00 | .18 | .00 | .00 | .59 | .00 |
| 12 | 1 | .780 | .00 | .00 | .00 | .00 | .01 | .88 | .00 |

| Bands | Degeneracy | E (Ry) | Os s | Os p | Os d | Ca s | Ca p | Ca d | H s |
|---|---|---|---|---|---|---|---|---|---|
| 1 | 1 | -.058 | .01 | .00 | .27 | .00 | .03 | .01 | .20 |
| 2,3 | 2 | -.001 | .00 | .00 | .41 | .00 | .00 | .00 | .20 |
| 4 | 1 | .114 | .00 | .05 | .00 | .08 | .00 | .03 | .21 |
| 5,6 | 2 | .196 | .00 | .05 | .00 | .00 | .05 | .00 | .26 |
| 7 | 1 | .254 | .00 | .00 | .56 | .05 | .00 | .03 | .00 |
| 8,9 | 2 | .292 | .00 | .00 | .66 | .00 | .01 | .05 | .00 |
| 10 | 1 | .533 | .00 | .00 | .36 | .00 | .01 | .17 | .01 |
| 11 | 1 | .604 | .00 | .00 | .00 | .00 | .00 | .70 | .00 |
| 12 | 1 | .665 | .00 | .00 | .16 | .04 | .00 | .57 | .00 |

values of the energy gap as a function of the unit cell volume. We observe an increase of $\Delta_g$ in the $Mg_2M'H_6$ series. On the other hand, the decrease of $\Delta_g$ in the $M_2FeH_6$ series is due to the presence of additional Ca d/Fe d states at the bottom of the conduction band. Experimental determinations of the energy gap are not yet available in the literature. As an indication, the colours of these materials are in agreement with the calculated $\Delta_g$ values. $Mg_2FeH_6$ is dark green while $Mg_2RuH_6$ is light green and $Mg_2OsH_6$ is almost white.

It is well known that the absolute values of energy gaps obtained within the local-density approach are not reliable. However, since in the present work we are mostly interested in discussing trends in the variation of energy gaps in a series of similar compounds, we do not expect our main conclusions to be affected.

## 4. Conclusions

We have calculated the band structure, DOS and partial wave analysis of the $M_2M'H_6$ intermetallic hydrides by means of the APW method. These hydrides appear to be semiconductors with an indirect energy gap. We found that the increase of the energy gap in the Mg series is mainly due to the splitting between the M' $d_{e_g}$ bonding and antibonding states, which results from the increase of the atomic number of the transition metal.

In the Ca and Sr series, new states are induced by the Ca d (or Sr d) orbitals which modify the nature of the energy gap. The presence of these new M' d/Ca d (or M' d/Sr d) states above the Fermi energy reduces the the value of the energy gap. These states could be observed by x-ray absorption spectroscopy by measuring the electronic transition Ca (or Sr) $L_{III}$.

## References

Belin E, Gupta M, Zolliker P and Yvon K 1987 *J. Less-Common Met.* **130** 267

Didisheim J J, Zolliker P, Yvon K, Fischer P, Schefer J, Gubelmann M and Williams A F 1984 *Inorg. Chem.* **23** 1953

Gupta M 1984 *J. Less-Common Met.* **103** 325
Gupta M, Belin E and Schlapbach L 1984 *J. Less-Common Met.* **103** 389
Gupta M and Schlapbach L 1988 *Hydrogen in Intermetallic Compounds I (Topics in Applied Physics 63)* ed L Schlapbach (Berlin: Springer)
Huang B, Bonhomme F, Selvam P, Yvon K and Fischer P 1991 *J. Less-Common Met.* **171** 301
Kritikos M, Noréus D, Bogdanović B and Wilczok U 1990 *J. Less-Common Met.* **161** 337
Lehmann G and Taut M 1972 *Phys. Status Solidi* b **54** 469
Lindsay R, Moyer R O Jr and Storey D F 1989 *Z. Phys. Chem., NF* **163** 309
Mattheiss L C, Wood J H and Switendick A C 1968 *Methods in Computational Physics* vol 8, ed B Adler, S Fernbach and M Rotenberg (New York: Academic)
Moyer R O Jr, Stanitsky C, Tanaka J, Kay M Y and Kleinberg J R 1971 *J. Solid State Chem.* **3** 541
Orgaz E and Gupta M 1987 *J. Less-Common Met.* **130** 293
—— 1993 *Z. Phys. Chem., NF* at press
Reilly J J and Wiswall R H 1968 *Inorg. Chem.* **7** 2254
Slater J C 1951 *Phys. Rev.* **81** 385
Von Barth U and Hedin L 1972 *J. Phys. C: Solid State Phys.* **5** 1629
Zhuang J, Hastings J M, Corliss L M, Bau R, Chiau-Yu Wei and Moyer R O 1981 *J. Solid State Chem.* **40** 352
Zolliker P, Yvon K, Fischer P and Schefer J 1985 *Inorg. Chem.* **24** 4177